

doi: 10.19388/j.zgdzdc.2023.05.09

引用格式: 王存智,张翔,黄志忠,等.安徽省贵池地区中生代闪长玢岩脉捕获锆石年龄对江南过渡带基底性质的制约[J].中国地质调查,2023,10(5):71-81.(Wang C Z,Zhang X,Huang Z Z,et al.The constraints of captured zircon ages from Mesozoic diorite porphyrite vein in Guichi area of Anhui Province on the basement nature of Jiangnan transitional zone[J].Geological Survey of China,2023,10(5):71-81.)

安徽省贵池地区中生代闪长玢岩脉捕获锆石年龄对江南过渡带基底性质的制约

王存智,张翔,黄志忠,宋世明,鞠冬梅,褚平利

(中国地质调查局南京地质调查中心,江苏南京 210016)

摘要:江南过渡带位于下扬子地区江南造山带北缘,为了探讨江南过渡带的基底性质,对贵池地区化芝里村中生代闪长玢岩脉中的捕获锆石进行了U-Pb测年和Hf同位素分析。结果显示:贵池地区闪长玢岩脉锆石年龄分布较为分散,其中5颗原生锆石的加权平均年龄为 (147.7 ± 2.2) Ma,指示了岩脉的形成年龄;捕获锆石中除一颗古太古代锆石年龄为 $(3\ 263 \pm 44)$ Ma外,其余锆石年龄主要分布在850~712 Ma、1 346~1 139 Ma、2 283~1 828 Ma及2 944~2 302 Ma,与长江中下游平原发育的董岭岩群碎屑锆石的年龄分布一致。贵池地区闪长玢岩脉锆石的Hf同位素组成也与董岭岩群、崆岭岩群的岩石类似,与江南造山带基底岩石存在较大差别,指示了本区存在“江北式”基底,同时表明常州—崇阳断裂不适合作为下扬子地区“江北式”和“江南式”基底的界线,推测界线位于更靠南侧的江南断裂。研究有助于加深对下扬子地区构造格局的理解。

关键词:江南过渡带;基底性质;闪长玢岩;锆石U-Pb测年;Hf同位素

中图分类号: P597 **文献标志码:** A **文章编号:** 2095-8706(2023)05-0071-11

0 引言

下扬子地区具有“一盖多底”的特征^[1],前人根据基底物质成分的差异,通常以崇阳—常州断裂为界将下扬子地区划分为“江南式”和“江北式”两种基底^[1-2]。崇阳—常州断裂以南的“江南式”基底以江南造山带的新元古代浅变质岩及花岗岩为代表,断裂以北的“江北式”基底在长江中下游平原以江西星子杂岩和安徽董岭岩群为代表。但由于下扬子地区被古生界—中生界的巨厚沉积覆盖,董岭岩群出露较少,目前研究对于“江北式”基底分布范围和性质的认识远不如“江南式”基底^[3]。此外,前人对下扬子地区最古老基底时代和组成的推测来自中生代岩浆岩中零星分布的捕获锆石或继承锆石的年龄信息^[4-8],但这些数

据尚不足以阐明其物质来源和基底信息。

本文在安徽省贵池地区化芝里村新发现了一处闪长玢岩脉,在岩脉中采集了锆石样品,通过对样品开展U-Pb测年及Hf同位素分析,确定其形成时代和物质来源,研究可为理解江南过渡带基底性质提供依据。

1 区域地质概况及样品特征

下扬子地区处于扬子板块东部,其北西以郟庐断裂为界与大别造山带、华北板块相邻,南以江山—绍兴断裂为界与华夏板块接壤^[9]。下扬子地区一般以崇阳—常州断裂为界分为长江中下游平原和江南隆起带两个构造单元^[10-11],而江南隆起带包括新元古代基底广泛出露的江南造山带及其与

收稿日期: 2023-03-07; 修订日期: 2023-08-23。

基金项目: 中国地质调查局“重要陆块区区域地质调查(编号: DD20221633)”及“东南沿海火山岩区区域地质调查(编号: DD20230212)”项目联合资助。

第一作者简介: 王存智(1983—),男,正高级工程师,主要从事构造地质调查工作。Email: 32107407@qq.com。

通信作者简介: 张翔(1988—),男,高级工程师,主要从事火山岩及地质遗迹调查工作。Email: 394264845@qq.com。

长江中下游平原之间的江南过渡带,两者之间被江南断裂分开(图 1(a))^[9]。

下扬子地区的地层主要由元古宇中—低级变质岩系、寒武系—中三叠统海相碳酸盐岩和碎屑岩、上三叠统一侏罗系陆相碎屑岩以及白垩系火山岩、红层等组成^[9]。其中火山岩均形成于早白垩世,成岩时代为 135 ~ 125 Ma^[8,12-17]。侵入岩广泛发育,

成岩时代为 152 ~ 101 Ma^[18-19]。

化芝里村位于江南过渡带内的贵池地区(图 1(b)),区内以早古生代沉积为主,NE 向褶皱及断裂构造发育。燕山期岩浆作用强烈,早期(148 ~ 136 Ma)以花岗闪长岩、闪长岩类为主,一般为小规模的斑岩,晚期(130 ~ 125 Ma)以规模较大的 A 型花岗岩类为主^[20]。

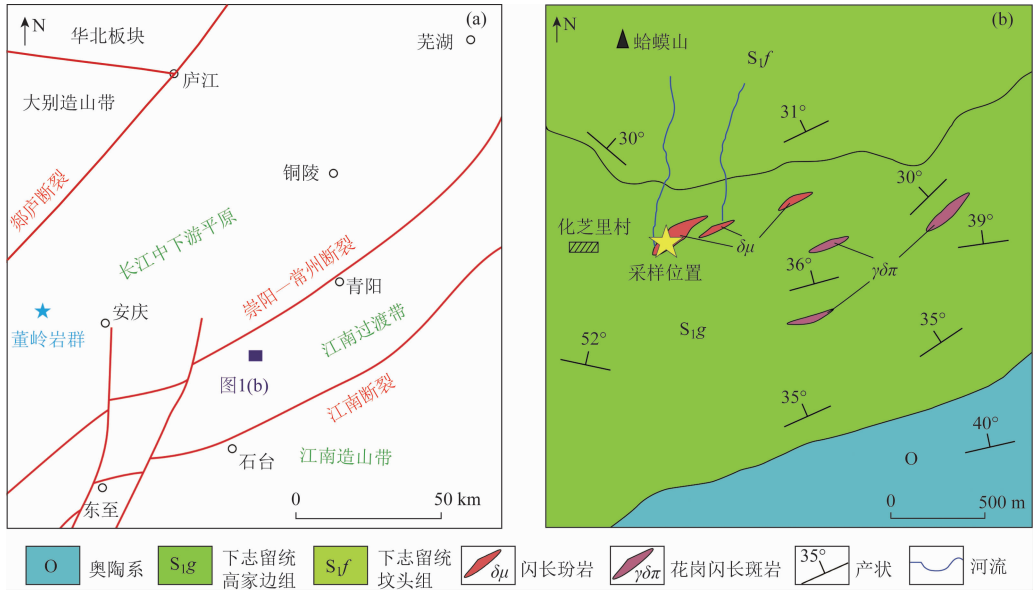


图 1 下扬子地区构造单元略图(a)^[11]及贵池地区地质简图(b)

Fig.1 Tectonic sketch of Lower Yangtze area (a)^[11] and geological sketch of Guichi area (b)

化芝里村发育的闪长玢岩脉在河道内出露较好,在河岸上可见岩脉沿志留系高家边组顺层侵入的接触界线(图 2(a)),志留统砂岩具有弱角岩化现象。闪长玢岩样品(D1804)采于河沟之中(图 2(b)),样品为斑状结构,块状构造,斑晶主要为斜长石、角闪石和少量黑云母,基质主要为斜长石。

显微镜下观察显示:斑晶斜长石(10%)呈半自形粒状,大多具有钠黝帘石化特征;角闪石(7%)呈自形一半自形柱状,大多具有绿泥石化特征;黑云母(3%)呈半自形片状,绿泥石化发育;基质(80%)主要为隐晶质斜长石,整体发育碳酸盐化(图 2(c),(d))。

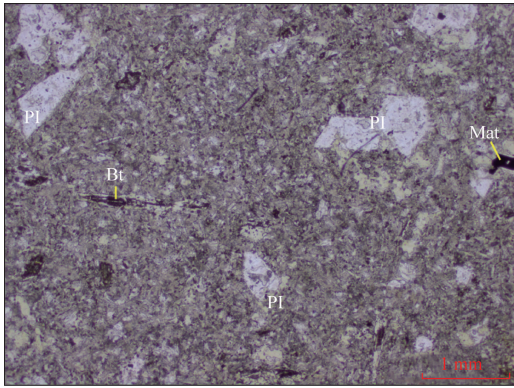


(a) 化芝里闪长玢岩脉野外露头

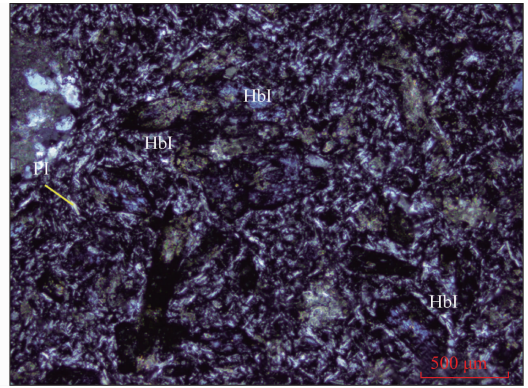
(b) 闪长玢岩手标本

图 2-1 贵池地区闪长玢岩野外及镜下照片

Fig.2-1 Field and microscope photos of diorite porphyrytes in Guichi area



(c) 闪长玢岩单偏光镜下特征



(d) 闪长玢岩正交偏光镜下特征

Pl. 斜长石; Hbl. 角闪石; Bt. 黑云母; Mat. 磁铁矿

图 2-2 贵池地闪长玢岩野外及镜下照片

Fig. 2-2 Field and microscope photos of diorite porphyrites in Guichi area

2 分析测试方法

锆石分选和阴极发光照相由南京宏创地质勘查技术服务有限公司完成,使用环氧树脂制靶之后拍摄阴极发光(cathodoluminescence, CL)图像。锆石 U - Pb 测年由中山大学广东省海洋资源与近岸工程重点实验室完成,采用激光剥蚀电感耦合等离子体质谱仪 LA - ICP - MS 分析,激光剥蚀束斑直径为 35 μm 。测试数据由 ICPMS DataCal 软件处理完成^[21-22],锆石 U - Pb 年龄谱和图绘制和加权平均年龄计算采用 Isoplot 3.0^[23]完成。

锆石 Hf 同位素测试由南京大学内生金属矿床成矿机制研究国家重点实验室完成。所用仪器为 New Wave UP193 激光剥蚀系统及其相连接的 Thermo Neptune Plus 多接收等离子体质谱仪,激光束斑直径为 44 μm ,采用 MT 作为外部标样,¹⁷⁶Hf/¹⁷⁷Hf 比值为 0.282 530 \pm 0.000 030。 $\epsilon_{\text{Hf}}(t)$ 计算

采用的¹⁷⁶Lu 的衰变常数为 1.865×10^{-11} ^[24],球粒陨石的¹⁷⁶Hf/¹⁷⁷Hf = 0.282 772,¹⁷⁶Lu/¹⁷⁷Hf = 0.033 2^[25]。亏损地幔 Hf 模式年龄(t_{DM1})采用¹⁷⁶Hf/¹⁷⁷Hf = 0.283 251,¹⁷⁶Lu/¹⁷⁷Hf = 0.038 4^[26],二阶段 Hf 模式年龄(t_{DM2})采用平均大陆壳¹⁷⁶Lu/¹⁷⁷Hf = 0.015 计算^[27]。

3 分析结果

3.1 锆石 U - Pb 年龄

闪长玢岩脉样品中锆石数量丰富,锆石颗粒直径介于 50 ~ 200 μm ,锆石形态结构呈短柱状、粒状、不规则状等,除少数为自形一半自形外,大部分呈中等一较高度度的磨圆。在锆石 CL 图像上可以看到,锆石内部有的可见显著的核幔结构、条纹状结构和岩浆震荡环带结构(图 3)。这些锆石结构特征反映了锆石来源的多样性,且锆石在形成后可能经历了复杂的地质作用过程。

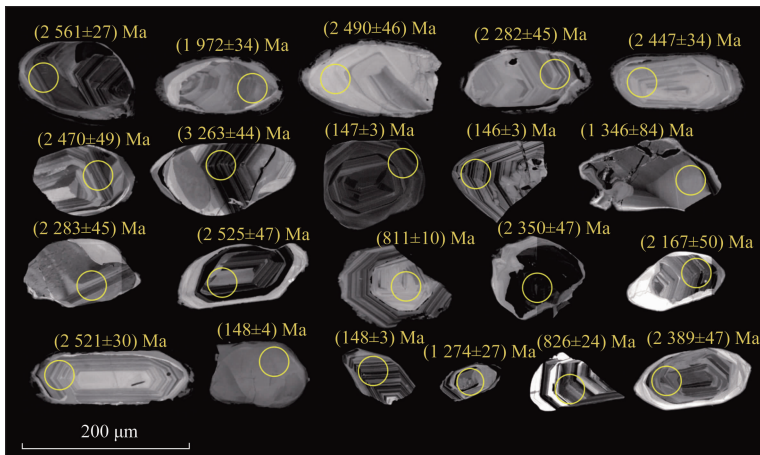


图 3 贵池地区闪长玢岩锆石 CL 图像

Fig. 3 Zircon CL images of diorite porphyrite in Guichi area

本文对闪长玢岩脉样品中的 120 颗锆石开展了 U - Pb 测年, 获得了 102 个有效数据, 测试结果见表 1 和表 2。锆石样品的 Th、U 含量分别为 $(29.8 \sim 490) \times 10^{-6}$ 和 $(30.6 \sim 3142) \times 10^{-6}$, Th/U 比值介于 0.1 ~ 1.8, 指示了岩浆锆石成因。在锆石 U - Pb 年龄谐和图上, 本次测试的 102 个数据点均

落在谐和线上(图 4), 且分布较为分散。对于年龄大于 1 000 Ma 的锆石年龄本文选择 $^{207}\text{Pb}/^{206}\text{Pb}$ 年龄(表 1), 小于 1 000 Ma 的锆石年龄选择 $^{206}\text{Pb}/^{238}\text{U}$ 年龄(表 2)。5 颗原生锆石的年龄介于 151 ~ 144 Ma, 加权平均年龄为 (147.7 ± 2.2) Ma (NSWD = 0.85, 图 4), 指示了岩脉的形成年龄。

表 1 贵池地区闪长玢岩脉 $^{207}\text{Pb}/^{206}\text{Pb}$ 年龄数据

Tab. 1 Zircon $^{207}\text{Pb}/^{206}\text{Pb}$ ages of diorite porphyrite vein in Guichi area

点号	元素含量/ 10^{-6}		Th/U	同位素比值及误差			年龄及误差/Ma	
	Th	U		$^{207}\text{Pb}/^{206}\text{Pb} \pm 1\sigma$	$^{207}\text{Pb}/^{235}\text{U} \pm 1\sigma$	$^{206}\text{Pb}/^{238}\text{U} \pm 1\sigma$	$^{207}\text{Pb}/^{235}\text{U} \pm 1\sigma$	$^{207}\text{Pb}/^{206}\text{Pb} \pm 1\sigma$
1	71.5	164.5	0.43	0.155 6 ± 0.003 1	7.910 1 ± 0.187 9	0.366 7 ± 0.006 5	2 221 ± 21	2 409 ± 33
2	265.7	211.2	1.26	0.170 3 ± 0.002 8	10.411 2 ± 0.176 2	0.440 9 ± 0.004 6	2 472 ± 16	2 561 ± 27
3	67.9	47.9	1.42	0.142 1 ± 0.002 6	8.309 3 ± 0.157 7	0.423 3 ± 0.005 2	2 265 ± 17	2 254 ± 32
4	44.7	30.6	1.46	0.181 2 ± 0.003 6	11.952 6 ± 0.257 4	0.477 3 ± 0.006 9	2 601 ± 20	2 665 ± 32
5	141.8	153.2	0.93	0.121 0 ± 0.002 3	5.760 0 ± 0.119 4	0.343 2 ± 0.004 3	1 940 ± 18	1 972 ± 34
6	88.1	140.0	0.63	0.160 2 ± 0.003 6	10.160 7 ± 0.237 5	0.458 0 ± 0.006 4	2 450 ± 22	2 458 ± 37
7	119.0	86.7	1.37	0.163 4 ± 0.003 8	10.137 6 ± 0.238 7	0.448 0 ± 0.005 9	2 447 ± 22	2 491 ± 39
8	45.1	44.9	1.00	0.163 3 ± 0.004 5	10.298 0 ± 0.283 7	0.456 0 ± 0.006 7	2 462 ± 26	2 490 ± 46
9	100.3	92.5	1.08	0.144 6 ± 0.003 7	7.714 6 ± 0.199 2	0.385 1 ± 0.005 4	2 198 ± 23	2 283 ± 45
10	254.6	189.4	1.34	0.162 2 ± 0.003 7	10.168 6 ± 0.231 9	0.451 5 ± 0.005 5	2 450 ± 21	2 480 ± 38
11	81.0	80.1	1.01	0.130 5 ± 0.002 9	7.045 6 ± 0.163 0	0.389 4 ± 0.005 1	2 117 ± 21	2 106 ± 39
12	89.8	122.7	0.73	0.159 2 ± 0.003 2	10.303 0 ± 0.232 0	0.465 7 ± 0.006 7	2 462 ± 21	2 447 ± 34
13	141.3	149.5	0.95	0.159 7 ± 0.003 0	9.885 7 ± 0.197 6	0.445 2 ± 0.005 3	2 424 ± 18	2 454 ± 32
14	44.7	54.3	0.82	0.166 5 ± 0.003 7	10.643 5 ± 0.241 9	0.463 4 ± 0.007 5	2 493 ± 21	2 524 ± 37
15	90.4	55.3	1.63	0.166 3 ± 0.003 0	10.838 9 ± 0.197 4	0.470 0 ± 0.006 0	2 509 ± 17	2 521 ± 30
16	225.2	268.6	0.84	0.159 0 ± 0.002 7	9.771 3 ± 0.184 1	0.442 9 ± 0.006 6	2 413 ± 17	2 456 ± 28
17	217.3	215.8	1.01	0.156 5 ± 0.002 6	8.235 3 ± 0.150 6	0.378 3 ± 0.005 0	2 257 ± 17	2 418 ± 28
18	225.9	340.0	0.66	0.157 0 ± 0.002 8	9.678 6 ± 0.187 2	0.443 2 ± 0.006 0	2 405 ± 18	2 433 ± 31
19	272.0	258.3	1.05	0.177 1 ± 0.002 7	11.209 2 ± 0.178 9	0.455 6 ± 0.005 3	2 541 ± 15	2 626 ± 26
20	141.3	124.5	1.13	0.157 3 ± 0.002 3	9.062 9 ± 0.137 2	0.415 2 ± 0.004 6	2 344 ± 14	2 428 ± 25
21	219.0	258.0	0.85	0.157 4 ± 0.002 2	9.318 1 ± 0.136 7	0.425 6 ± 0.004 2	2 370 ± 14	2 428 ± 23
22	46.8	118.9	0.39	0.127 7 ± 0.002 2	5.530 6 ± 0.103 0	0.312 6 ± 0.003 8	1 905 ± 16	2 066 ± 32
23	199.6	157.8	1.27	0.135 9 ± 0.002 0	6.862 0 ± 0.108 8	0.364 0 ± 0.004 1	2 094 ± 14	2 173 ± 25
24	411.4	276.6	1.49	0.180 9 ± 0.002 6	11.584 0 ± 0.187 4	0.461 6 ± 0.005 9	2 571 ± 15	2 661 ± 23
25	35.4	65.9	0.54	0.125 0 ± 0.002 7	5.125 7 ± 0.117 0	0.295 9 ± 0.004 4	1 840 ± 19	2 029 ± 38
26	58.1	144.0	0.40	0.161 4 ± 0.004 7	10.064 3 ± 0.281 9	0.444 6 ± 0.005 6	2 441 ± 26	2 470 ± 49
27	161.0	341.0	0.47	0.154 4 ± 0.004 2	8.642 0 ± 0.232 0	0.398 3 ± 0.005 2	2 301 ± 24	2 395 ± 45
28	132.0	171.0	0.77	0.160 1 ± 0.004 2	10.504 3 ± 0.255 0	0.469 4 ± 0.005 7	2 480 ± 23	2 457 ± 44
29	68.3	106.0	0.65	0.154 7 ± 0.004 3	8.516 3 ± 0.233 8	0.392 3 ± 0.004 9	2 288 ± 25	2 399 ± 52
30	273.0	416.0	0.66	0.142 9 ± 0.003 5	8.230 4 ± 0.197 4	0.410 0 ± 0.004 2	2 257 ± 22	2 263 ± 43
31	91.9	207.0	0.45	0.154 8 ± 0.004 5	10.014 8 ± 0.333 9	0.460 3 ± 0.009 3	2 436 ± 31	2 400 ± 50
32	310.0	483.0	0.64	0.155 2 ± 0.004 2	8.987 3 ± 0.244 4	0.412 4 ± 0.005 0	2 337 ± 25	2 406 ± 46
33	76.5	133.0	0.57	0.215 0 ± 0.005 7	16.525 0 ± 0.434 2	0.549 4 ± 0.007 2	2 908 ± 25	2 944 ± 44
34	64.1	568.0	0.11	0.170 2 ± 0.004 3	10.011 6 ± 0.252 7	0.420 1 ± 0.004 5	2 436 ± 23	2 561 ± 43
35	103.0	214.0	0.48	0.164 2 ± 0.004 1	10.811 4 ± 0.275 9	0.470 5 ± 0.004 9	2 507 ± 24	2 499 ± 43
36	91.0	694.0	0.13	0.183 5 ± 0.004 6	12.156 6 ± 0.293 4	0.474 0 ± 0.005 3	2 617 ± 23	2 684 ± 42
37	490.0	730.0	0.67	0.165 4 ± 0.004 2	9.792 5 ± 0.247 3	0.423 3 ± 0.004 2	2 415 ± 23	2 522 ± 43
38	143.0	203.0	0.71	0.171 2 ± 0.004 8	10.694 2 ± 0.303 3	0.447 0 ± 0.005 1	2 497 ± 26	2 570 ± 46
39	62.7	170.0	0.37	0.164 7 ± 0.005 3	9.194 9 ± 0.301 9	0.401 3 ± 0.005 8	2 358 ± 30	2 506 ± 54
40	203.0	294.0	0.69	0.170 9 ± 0.005 3	9.484 2 ± 0.289 6	0.398 1 ± 0.005 1	2 386 ± 28	2 569 ± 52
41	336.0	379.0	0.89	0.167 4 ± 0.004 8	9.841 6 ± 0.286 8	0.420 6 ± 0.004 8	2 420 ± 27	2 532 ± 49
42	142.0	208.0	0.69	0.083 2 ± 0.003 3	2.032 8 ± 0.078 9	0.175 3 ± 0.002 5	1 127 ± 26	1 274 ± 77
43	47.2	202.0	0.23	0.175 1 ± 0.004 5	11.455 5 ± 0.298 0	0.467 2 ± 0.005 5	2 561 ± 24	2 607 ± 43

续表

点号	元素含量/ 10^{-6}		Th/U	同位素比值及误差			年龄及误差/Ma	
	Th	U		$^{207}\text{Pb}/^{206}\text{Pb} \pm 1\sigma$	$^{207}\text{Pb}/^{235}\text{U} \pm 1\sigma$	$^{206}\text{Pb}/^{238}\text{U} \pm 1\sigma$	$^{207}\text{Pb}/^{235}\text{U} \pm 1\sigma$	$^{207}\text{Pb}/^{206}\text{Pb} \pm 1\sigma$
44	110.0	340.0	0.32	0.163 4 ± 0.004 0	9.982 7 ± 0.243 1	0.436 2 ± 0.004 2	2 433 ± 22	2 491 ± 41
45	64.8	110.0	0.59	0.176 6 ± 0.005 1	12.388 1 ± 0.399 5	0.499 2 ± 0.008 0	2 634 ± 30	2 621 ± 48
46	49.6	97.0	0.51	0.163 7 ± 0.004 9	10.929 8 ± 0.326 1	0.478 2 ± 0.006 9	2 517 ± 28	2 494 ± 51
47	178.0	358.0	0.50	0.262 6 ± 0.007 3	21.798 7 ± 0.598 3	0.590 9 ± 0.006 5	3 175 ± 27	3 263 ± 44
48	103.0	239.0	0.43	0.150 2 ± 0.004 5	9.222 2 ± 0.272 8	0.438 2 ± 0.005 5	2 360 ± 27	2 350 ± 52
49	255.0	368.0	0.69	0.167 0 ± 0.004 4	10.657 5 ± 0.282 2	0.454 7 ± 0.005 0	2 494 ± 25	2 527 ± 44
50	103.0	138.0	0.74	0.121 7 ± 0.003 6	5.987 2 ± 0.184 2	0.350 4 ± 0.004 5	1 974 ± 27	1 981 ± 52
51	153.0	187.0	0.82	0.214 3 ± 0.006 0	15.097 1 ± 0.404 3	0.504 1 ± 0.006 5	2 821 ± 26	2 938 ± 46
52	58.8	330.0	0.18	0.204 8 ± 0.005 6	13.930 3 ± 0.375 1	0.485 9 ± 0.006 3	2 745 ± 26	2 865 ± 45
53	76.1	163.0	0.47	0.172 7 ± 0.005 6	10.932 1 ± 0.351 5	0.453 6 ± 0.005 3	2 517 ± 30	2 584 ± 55
54	72.1	132.0	0.55	0.086 3 ± 0.003 7	2.279 6 ± 0.096 0	0.191 5 ± 0.002 9	1 206 ± 30	1 346 ± 84
55	165.0	128.0	1.29	0.161 1 ± 0.005 8	9.733 8 ± 0.335 0	0.434 5 ± 0.006 6	2 410 ± 32	2 478 ± 61
56	75.3	141.0	0.53	0.175 0 ± 0.005 5	11.399 8 ± 0.352 3	0.467 7 ± 0.006 3	2 556 ± 29	2 606 ± 52
57	63.9	92.5	0.69	0.132 3 ± 0.004 5	7.398 6 ± 0.246 1	0.401 8 ± 0.005 3	2 161 ± 30	2 128 ± 55
58	37.1	1028.0	0.04	0.161 9 ± 0.004 5	10.072 5 ± 0.287 7	0.444 1 ± 0.005 1	2 441 ± 26	2 476 ± 48
59	246.0	401.0	0.62	0.165 4 ± 0.005 3	10.323 5 ± 0.319 4	0.446 2 ± 0.005 5	2 464 ± 29	2 522 ± 54
60	64.5	193.0	0.33	0.164 1 ± 0.005 5	10.159 1 ± 0.333 3	0.442 6 ± 0.005 2	2 449 ± 30	2 498 ± 56
61	169.0	162.0	1.04	0.077 6 ± 0.003 4	1.910 3 ± 0.080 2	0.176 5 ± 0.002 3	1 085 ± 28	1 139 ± 86
62	468.0	676.0	0.69	0.165 3 ± 0.005 4	10.144 6 ± 0.338 1	0.438 0 ± 0.005 8	2 448 ± 31	2 510 ± 55
63	158.0	393.0	0.4	0.146 1 ± 0.004 5	7.965 0 ± 0.242 9	0.389 6 ± 0.004 6	2 227 ± 28	2 302 ± 53
64	362.0	489.0	0.74	0.150 3 ± 0.004 2	8.997 4 ± 0.245 8	0.428 1 ± 0.004 3	2 338 ± 25	2 350 ± 47
65	247.0	300.0	0.82	0.166 7 ± 0.004 7	11.013 6 ± 0.297 5	0.474 3 ± 0.004 9	2 524 ± 25	2 525 ± 47
66	57.9	38.3	1.51	0.138 6 ± 0.005 6	8.229 0 ± 0.336 9	0.427 4 ± 0.007 0	2 257 ± 37	2 210 ± 70
67	194.0	160.0	1.21	0.162 1 ± 0.005 5	9.896 8 ± 0.328 9	0.437 9 ± 0.007 1	2 425 ± 31	2 477 ± 56
68	101.0	112.0	0.90	0.124 2 ± 0.004 3	6.481 9 ± 0.228 0	0.375 3 ± 0.005 6	2 043 ± 31	2 018 ± 62
69	253.0	217.0	1.17	0.164 1 ± 0.004 9	10.679 3 ± 0.313 1	0.467 6 ± 0.005 7	2 496 ± 27	2 498 ± 50
70	121.0	345.0	0.35	0.134 4 ± 0.003 8	7.016 3 ± 0.194 3	0.374 7 ± 0.003 9	2 114 ± 25	2 167 ± 50
71	29.8	271.0	0.11	0.128 9 ± 0.003 6	6.696 5 ± 0.184 7	0.373 0 ± 0.003 8	2 072 ± 24	2 083 ± 50
72	87.8	89.2	0.98	0.127 6 ± 0.004 5	5.975 3 ± 0.210 7	0.338 0 ± 0.005 5	1 972 ± 31	2 065 ± 31
73	53.6	88.0	0.61	0.167 8 ± 0.005 7	11.009 6 ± 0.372 5	0.471 2 ± 0.006 2	2 524 ± 32	2 536 ± 56
74	66.0	58.8	1.12	0.130 0 ± 0.005 3	6.523 5 ± 0.272 1	0.360 9 ± 0.006 6	2 049 ± 37	2 098 ± 72
75	159.0	162.0	0.98	0.124 1 ± 0.004 0	6.291 7 ± 0.203 5	0.362 4 ± 0.004 3	2 017 ± 28	2 017 ± 53
76	71.3	93.3	0.76	0.161 9 ± 0.005 3	10.769 6 ± 0.335 0	0.478 5 ± 0.008 2	2 503 ± 29	2 476 ± 55
77	57.4	383.0	0.15	0.163 6 ± 0.004 6	10.842 2 ± 0.331 7	0.473 8 ± 0.007 3	2 510 ± 28	2 494 ± 42
78	164.0	92.0	1.79	0.123 7 ± 0.004 8	6.264 5 ± 0.233 0	0.365 5 ± 0.005 4	2 013 ± 33	2 010 ± 69
79	147.0	145.0	1.01	0.123 2 ± 0.004 1	6.681 5 ± 0.219 0	0.390 3 ± 0.005 0	2 070 ± 29	2 003 ± 59
80	90.1	131.0	0.69	0.160 0 ± 0.005 0	10.245 2 ± 0.327 0	0.460 2 ± 0.006 3	2 457 ± 30	2 457 ± 54
81	57.8	124.0	0.47	0.173 4 ± 0.004 9	11.496 6 ± 0.334 8	0.476 5 ± 0.006 2	2 564 ± 27	2 590 ± 47
82	49.2	201.0	0.24	0.152 3 ± 0.004 5	9.619 1 ± 0.283 3	0.454 4 ± 0.005 3	2 399 ± 27	2 373 ± 50
83	147.0	186.0	0.79	0.162 5 ± 0.004 6	10.481 8 ± 0.315 4	0.463 8 ± 0.006 5	2 478 ± 28	2 483 ± 48
84	105.0	86.3	1.22	0.122 8 ± 0.004 3	6.237 3 ± 0.219 0	0.367 3 ± 0.005 5	2 010 ± 31	1 998 ± 62
85	82.2	158.0	0.52	0.181 1 ± 0.004 8	12.762 8 ± 0.352 4	0.506 6 ± 0.006 9	2 662 ± 26	2 665 ± 44
86	112.0	96.0	1.16	0.118 8 ± 0.004 1	6.136 6 ± 0.225 1	0.370 0 ± 0.005 9	1 995 ± 32	1 939 ± 61

表2 贵池地区闪长玢岩脉 $^{206}\text{Pb}/^{238}\text{Pb}$ 年龄数据

Tab.1 Zircon $^{206}\text{Pb}/^{238}\text{Pb}$ ages of diorite porphyrite vein in Guichi area

点号	元素含量/ 10^{-6}		Th/U	同位素比值及误差			年龄及误差/Ma	
	Th	U		$^{207}\text{Pb}/^{206}\text{Pb} \pm 1\sigma$	$^{207}\text{Pb}/^{235}\text{U} \pm 1\sigma$	$^{206}\text{Pb}/^{238}\text{U} \pm 1\sigma$	$^{207}\text{Pb}/^{235}\text{U} \pm 1\sigma$	$^{206}\text{Pb}/^{238}\text{Pb} \pm 1\sigma$
1	37.8	41.9	0.90	0.065 4 ± 0.001 5	1.216 8 ± 0.028 9	0.134 1 ± 0.001 7	808 ± 13	811 ± 10
2	140.0	116.0	1.21	0.063 1 ± 0.002 9	1.091 2 ± 0.047 6	0.124 1 ± 0.001 9	749 ± 23	754 ± 11
3	280.0	324.0	0.87	0.065 1 ± 0.002 4	1.064 8 ± 0.038 2	0.116 8 ± 0.001 7	736 ± 19	712 ± 10
4	141.0	389.0	0.36	0.054 7 ± 0.003 8	0.171 0 ± 0.011 5	0.022 9 ± 0.000 4	160 ± 10	146 ± 3
5	215.0	3142.0	0.07	0.051 3 ± 0.001 7	0.166 9 ± 0.005 5	0.023 4 ± 0.000 3	157 ± 5	149 ± 2

续表

点号	元素含量/ 10^{-6}		Th/U	同位素比值及误差			年龄及误差/Ma	
	Th	U		$^{207}\text{Pb}/^{206}\text{Pb} \pm 1\sigma$	$^{207}\text{Pb}/^{235}\text{U} \pm 1\sigma$	$^{206}\text{Pb}/^{238}\text{U} \pm 1\sigma$	$^{207}\text{Pb}/^{235}\text{U} \pm 1\sigma$	$^{206}\text{Pb}/^{238}\text{Pb} \pm 1\sigma$
6	179.0	592.0	0.30	0.049 3 ± 0.003 0	0.157 5 ± 0.009 4	0.023 3 ± 0.000 4	149 ± 8	148 ± 3
7	201.0	385.0	0.52	0.066 6 ± 0.002 4	1.267 9 ± 0.045 0	0.136 7 ± 0.001 6	831 ± 20	826 ± 9
8	54.7	318.0	0.17	0.058 2 ± 0.004 1	0.176 7 ± 0.011 9	0.022 6 ± 0.000 5	165 ± 10	144 ± 3
9	293.0	378.0	0.78	0.067 0 ± 0.003 1	1.277 4 ± 0.058 5	0.138 0 ± 0.002 4	836 ± 26	833 ± 14
10	78.2	200.0	0.39	0.066 9 ± 0.002 7	1.280 5 ± 0.056 2	0.137 0 ± 0.002 5	837 ± 25	828 ± 14
11	42.8	51.9	0.82	0.066 3 ± 0.005 1	1.221 8 ± 0.094 1	0.134 3 ± 0.003 4	811 ± 43	812 ± 19
12	116.0	93.0	1.25	0.070 1 ± 0.004 9	1.314 3 ± 0.083 2	0.137 9 ± 0.003 1	852 ± 37	833 ± 17
13	140.0	659.0	0.21	0.054 2 ± 0.003 5	0.178 0 ± 0.011 6	0.023 6 ± 0.000 6	166 ± 10	151 ± 4
14	140.0	203.0	0.69	0.063 4 ± 0.002 7	1.211 0 ± 0.051 6	0.137 7 ± 0.001 8	806 ± 24	832 ± 10
15	161.0	232.0	0.70	0.064 1 ± 0.002 6	1.193 9 ± 0.049 3	0.134 1 ± 0.001 9	798 ± 23	811 ± 11
16	180.0	170.0	1.06	0.066 9 ± 0.002 8	1.282 6 ± 0.052 0	0.138 6 ± 0.002 0	838 ± 23	837 ± 11

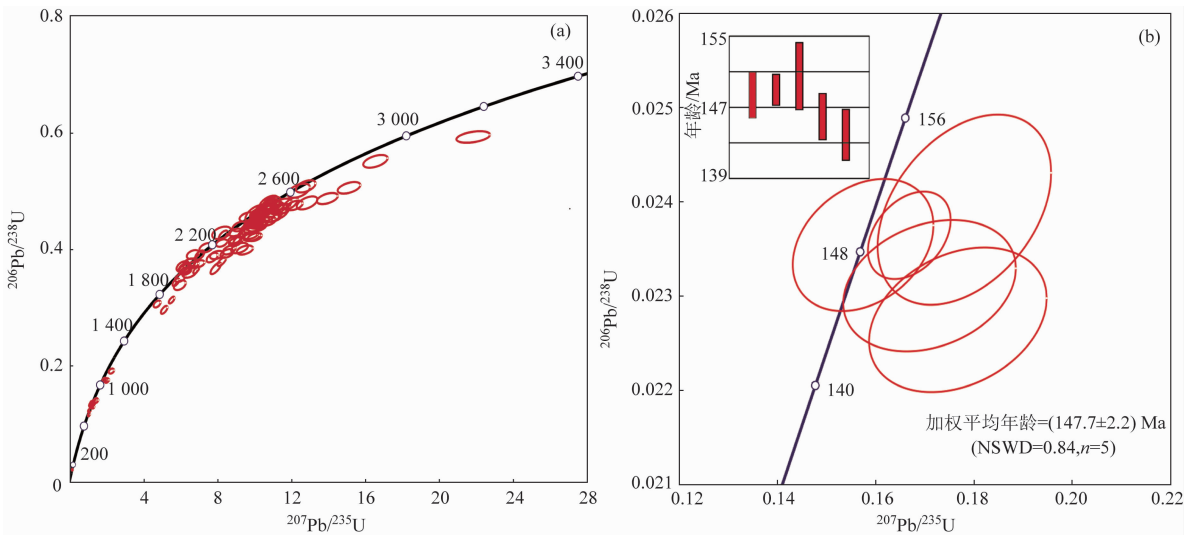


图 4 贵池地区闪长玢岩脉锆石 U - Pb 年龄谐和图 (a) 及原生锆石加权平均年龄 (b)

Fig. 4 Zircon U - Pb concordia diagram (a) and primary zircon weighted average age (b) of diorite porphyrite vein in the Guichi area

样品中除 5 颗原生锆石以外,其余锆石均为捕获锆石,其中一颗最古老的古太古代锆石的年龄为 (3 263 ± 44) Ma,其他捕获锆石年龄可以分为 4 组。第一组年龄为 850 ~ 712 Ma,分析数据点 11 个,年龄峰值约为 825 Ma; 第二组年龄为 1 346 ~ 1 139 Ma,分析数据点 3 个,加权平均年龄 (1 255 ± 95) Ma (NSWD = 1.5); 第三组年龄为 2 283 ~ 1 939 Ma,分析数据点 21 个,年龄峰值为

2 035 Ma; 第四组年龄为 2 944 ~ 2 302 Ma,分析数据点 62 个,年龄峰值为 2 450 Ma。

3.2 锆石 Hf 同位素

对样品 D1804 进行了 20 个点位锆石 Hf 同位素分析,测试结果见表 3。以测得的锆石 U - Pb 年龄进行计算, $(^{176}\text{Hf}/^{177}\text{Hf})_i$ 值为 0.280 934 ~ 0.281 404, $\varepsilon_{\text{Hf}}(t)$ 值为 -12.19 ~ -1.49, Hf 同位素模式年龄 t_{DM1} 为 3 153 ~ 2 530 Ma, t_{DM2} 为 3 690 ~ 2 925 Ma。

表 3 贵池地区闪长玢岩脉锆石 Hf 同位素数据

Tab. 3 Zircon Hf isotopic datas of diorite porphyrite vein in Guichi area

点号	U - Pb 年龄/Ma	$^{176}\text{Yb}/^{177}\text{Hf}$	$^{176}\text{Lu}/^{177}\text{Hf}$	$^{176}\text{Hf}/^{177}\text{Hf} \pm 1\sigma$	$(^{176}\text{Hf}/^{177}\text{Hf})_i$	$\varepsilon_{\text{Hf}}(t) \pm 1\sigma$	t_{DM1}/Ma	t_{DM2}/Ma
1	2 014	0.019 242	0.000 639	0.281 376 ± 0.000 007	0.281 352	-5.26 ± 0.25	2 597	2 989
2	2 354	0.018 900	0.000 688	0.281 029 ± 0.000 008	0.280 999	-10.02 ± 0.28	3 068	3 553
3	2 289	0.019 523	0.000 784	0.281 069 ± 0.000 007	0.281 035	-10.23 ± 0.25	3 022	3 516
4	2 276	0.022 531	0.000 908	0.281 328 ± 0.000 008	0.281 289	-1.49 ± 0.28	2 680	2 952
5	2 515	0.023 283	0.000 837	0.281 154 ± 0.000 008	0.281 114	-2.21 ± 0.28	2 911	3 182
6	1 902	0.009 454	0.000 347	0.281 241 ± 0.000 011	0.281 229	-12.19 ± 0.39	2 758	3 339

续表

点号	U - Pb 年龄/Ma	$^{176}\text{Yb}/^{177}\text{Hf}$	$^{176}\text{Lu}/^{177}\text{Hf}$	$^{176}\text{Hf}/^{177}\text{Hf} \pm 1\sigma$	$(^{176}\text{Hf}/^{177}\text{Hf})_i$	$\varepsilon_{\text{Hf}}(t) \pm 1\sigma$	t_{DM1}/Ma	t_{DM2}/Ma
7	2 243	0.016 329	0.000 613	0.281 224 ± 0.000 009	0.281 197	-5.50 ± 0.32	2 801	3 182
8	2 431	0.010 088	0.000 386	0.281 029 ± 0.000 013	0.281 011	-7.80 ± 0.46	3 045	3 472
9	2 422	0.012 088	0.000 486	0.281 049 ± 0.000 013	0.281 026	-7.46 ± 0.46	3 026	3 444
10	1 721	0.017 552	0.000 615	0.281 424 ± 0.000 009	0.281 404	-10.08 ± 0.32	2 530	3 066
11	2 100	0.022 794	0.000 790	0.281 304 ± 0.000 009	0.281273	-6.10 ± 0.32	2 704	3 109
12	2 120	0.009 624	0.000 362	0.281 322 ± 0.000 007	0.281 307	-4.41 ± 0.25	2 651	3 017
13	2 465	0.015 207	0.000 614	0.281 026 ± 0.000 008	0.280 997	-7.53 ± 0.28	3 067	3 481
14	2 455	0.022 855	0.000 796	0.280 989 ± 0.000 012	0.280 952	-9.34 ± 0.42	3 130	3 588
15	2 364	0.017 851	0.000 664	0.280 964 ± 0.000 008	0.280 934	-12.08 ± 0.28	3 153	3 690
16	2 068	0.025 824	0.000 961	0.281 194 ± 0.000 011	0.281 156	-10.98 ± 0.39	2 867	3 392
17	2 365	0.027 723	0.001 076	0.281 102 ± 0.000 009	0.281 053	-7.82 ± 0.32	3 000	3 422
18	2 420	0.019 238	0.000 745	0.281 124 ± 0.000 006	0.281 090	-5.26 ± 0.21	2 945	3 303
19	2 286	0.024 414	0.000 931	0.281 229 ± 0.000 009	0.281 188	-4.83 ± 0.32	2 817	3 172
20	2 001	0.016 899	0.000 628	0.281 408 ± 0.000 012	0.281 384	-4.41 ± 0.42	2 553	2 925

4 讨论

4.1 闪长玢岩脉形成时代

长江中下游平原广泛发育燕山期岩浆活动,可以划分为4个阶段:第一阶段148~136 Ma,产物主要为发育在鄂东南、九瑞、铜陵、安庆等隆起区的侵入岩,以高钾钙碱性系列的中酸性岩为主,岩石类型包括辉石闪长(二长)岩-石英闪长(二长)岩-花岗闪长岩,与区内铜、金多金属成矿密切相关^[9,28-35];第二阶段135~127 Ma,岩浆活动主要发生在凹陷区,包括金牛、怀宁、庐枞、繁昌、宁芜、溧阳和溧水盆地的火山岩及次火山岩^[8,12-15,36-37],与玢岩铁矿关系密切;第三阶段127~123 Ma,岩浆岩同时发育于隆起区和凹陷区,岩石类型以正长花岗岩和正长岩为主,属于A型花岗岩,与小规模的热液型金矿和铀矿有关^[38];第四阶段109~102 Ma,岩浆活

动仅发育在宁镇地区,岩石类型以闪长岩-二长岩-花岗岩为主,与铜、金多金属成矿相关^[39]。

本文获得的闪长玢岩脉样品中原生锆石的年龄为(147.7 ± 2.2) Ma,代表了其形成年龄,应为长江中下游平原燕山期第一阶段岩浆活动的产物。该期岩浆岩普遍具有高 Sr/Y 值、低 Y 以及富集 Sr-Nd 同位素的特征,因此被认为形成于挤压转为拉张的构造背景下,由热的玄武岩浆底侵引起下地壳加厚或拆沉,并发生部分熔融^[4,40]。

4.2 化里闪长玢岩的物源

贵池地区闪长玢岩脉捕获锆石年龄谱显示(图5(a)),锆石年龄有两个明显的峰值825 Ma和2450 Ma,及一个次峰2035 Ma。其中新元古代锆石年龄峰值可能与扬子板块新元古代大规模花岗质岩浆活动密切相关,而古元古代锆石的比例占大多数,与董岭岩群变质岩碎屑锆石的年龄相似(图5(b)),暗示董岭岩群可能为其物源。

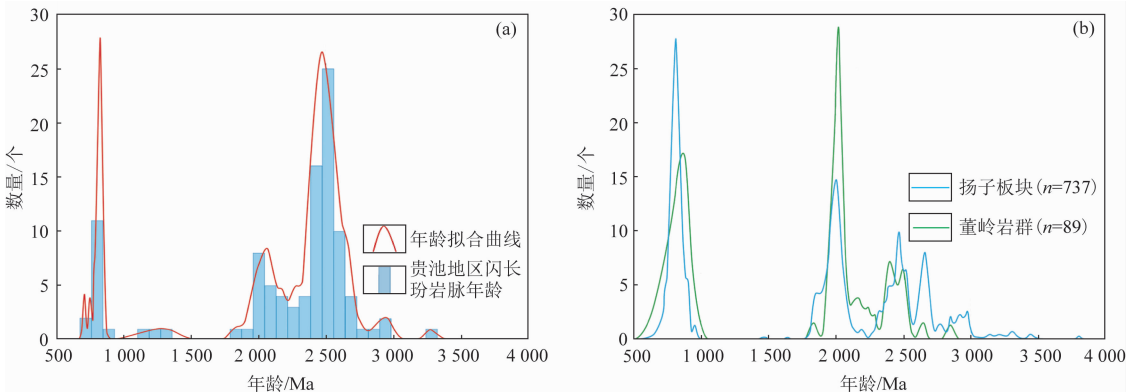


图5 贵池地区闪长玢岩脉捕获锆石年龄谱(a)及扬子板块和董岭岩群碎屑锆石年龄谱^[41](b)

Fig.5 Cumulative probability of captured zircon ages for diorite porphyrite vein in Guichi area

(a) and detrital zircon ages in Yangtze Plate and Dongling Complex^[41](b)

董岭岩群作为长江中下游成矿带出露较少的基底变质岩系之一,长期以来得到众多学者的关注。邢凤鸣等^[42]获得董岭岩群中斜长角闪岩的Sm-Nd等时线年龄为 $(1\ 895 \pm 72)$ Ma; Grimmer等^[43]通过单颗粒锆石蒸发法获得董岭岩群中钾长片麻岩的3组较为集中的年龄数据分别为 $(2\ 377 \pm 10) \sim (2\ 370 \pm 2)$ Ma、 $(2\ 016 \pm 6) \sim (1\ 971 \pm 6)$ Ma和 $(783 \pm 7) \sim (692 \pm 10)$ Ma,并认为第一组年龄可能指示了原岩形成时代,而后两组年龄可能代表了扬子板块基底固结时经历后期构造热事件改造的时代。Zhang等^[41]和Chen等^[3]通过对董岭岩群

的锆石开展U-Pb-Hf-O同位素研究,认为董岭岩群具有双层基底的物质表现形式,即在古元古代变质基底上覆盖了新元古代变质沉积盖层。

研究区闪长玢岩脉锆石Hf同位素的 $\varepsilon_{\text{Hf}}(t)$ 值范围为 $-12.19 \sim -1.49$,按照平均地壳的 $^{177}\text{Lu}/^{176}\text{Hf}$ 值(0.015)演化至820 Ma时,均低于江南造山带新元古代花岗岩的锆石Hf同位素组成,而与董岭岩群中的锆石Hf同位素组成相似(图6)。在锆石年龄- $\varepsilon_{\text{Hf}}(t)$ 图解中,研究区样品几乎都落入了董岭岩群锆石Hf同位素组成范围内,进一步表明贵池地区闪长玢岩脉来自于崆岭岩群和董岭岩群的古老地壳再造。

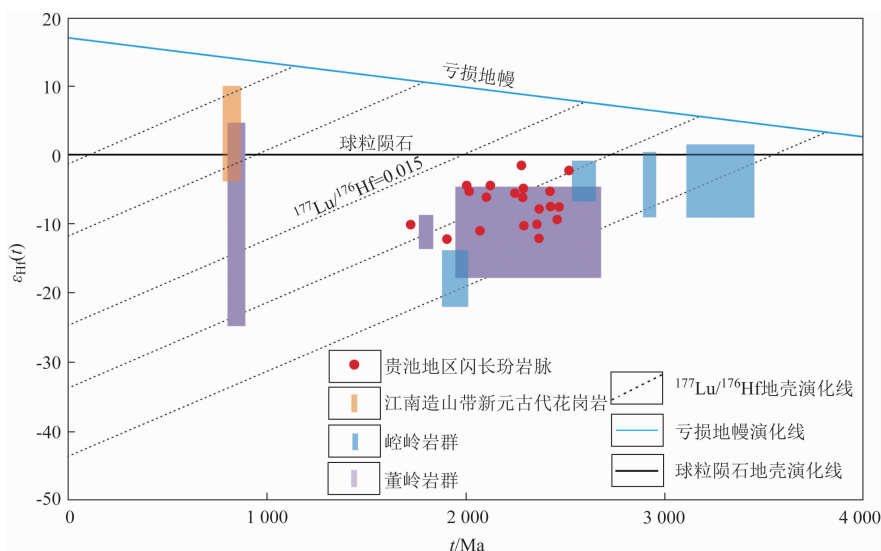


图6 贵池地区闪长玢岩锆石年龄- $\varepsilon_{\text{Hf}}(t)$ 图解^[3,41-42,44-46]

Fig. 6 Zircon ages - $\varepsilon_{\text{Hf}}(t)$ diagram of diorite porphyrite in Guichi area^[3,41-42,44-46]

4.3 捕获锆石对江南过渡带基底性质的制约

下扬子地区可分为以新元古代浅变质岩及花岗岩为代表的“江南式”基底和以江西星子杂岩和安徽董岭岩群为代表的“江北式”基底^[1-2]。近年的研究表明,星子杂岩可能是“江南式”基底的组成部分^[47-49],主要形成于新元古代^[50],而非古元古代^[51]。

“江北式”和“江南式”基底之间的界线通常被认为是常州—崇阳断裂(中段为高坦断裂)^[1-2],倘若如此,位于高坦断裂与江南断裂之间的江南过渡带应为“江南式”基底。但贵池地区闪长玢岩脉中捕获锆石的U-Pb年龄及Hf同位素组成指示了崆岭岩群和董岭岩群的特征,即“江北式”基底。因此,本文推测“江北式”基底和“江南式”基底之间的界线可能位于更靠南的江南断裂(图1)。

5 结论

(1) 贵池地区闪长玢岩脉中原生锆石的年龄为 (147.7 ± 2.2) Ma,代表了其形成年龄,为长江中下游平原燕山期第一阶段岩浆活动的产物。

(2) 捕获锆石的U-Pb年龄及Hf同位素组成表明化芝里闪长玢岩脉来自于崆岭岩群和董岭岩群的古老地壳再造,据此推测下扬子地区“江北式”基底和“江南式”基底之间界线可能为江南断裂。

参考文献(References):

- [1] 常印佛,董树文,黄德志.论中一下扬子“一盖多底”格局与演化[J].火山地质与矿产,1996,17(1/2):1-15.
Chang Y F, Dong S W, Huang D Z. On tectonics of “poly-base-ment with one cover” in Middle-Lower Yangtze craton China[J].

- Volcanology and Mineral Resources, 1996, 17(1/2): 1 - 15.
- [2] 董树文, 马立成, 刘刚, 等. 论长江中下游成矿动力学[J]. 地质学报, 2011, 85(5): 612 - 625.
Dong S W, Ma L C, Liu G, et al. On dynamics of the metallogenic belt of middle - lower reaches of Yangtze River, Eastern China[J]. Acta Geologica Sinica, 2011, 85(5): 612 - 625.
- [3] Chen Z H, Xing G F. Geochemical and zircon U - Pb - Hf - O isotopic evidence for a coherent Paleoproterozoic basement beneath the Yangtze Block, South China[J]. Precambrian Research, 2016, 279: 81 - 90.
- [4] 张旗, 简平, 刘敦一, 等. 宁芜火山岩的锆石 SHRIMP 定年及其意义[J]. 中国科学(D辑), 2003, 46(8): 830 - 837.
Zhang Q, Jian P, Liu D Y, et al. SHRIMP dating of volcanic rocks from Ningwu area and its geological implications[J]. Science in China Series D: Earth Sciences, 2003, 46(8): 830 - 837.
- [5] 王彦斌, 刘敦一, 曾普胜, 等. 铜陵地区小铜官山石英闪长岩锆石 SHRIMP 的 U - Pb 年龄及其成因指示[J]. 岩石矿物学杂志, 2004, 23(4): 298 - 304.
Wang Y B, Liu D Y, Zeng P S, et al. SHRIMP U - Pb geochronology of Xiaotongguanshan quartz - dioritic intrusions in Tongling district and its petrogenetic implications[J]. Acta Petrologica et Mineralogica, 2004, 23(4): 298 - 304.
- [6] 吴淦国, 张达, 狄永军, 等. 铜陵矿集区侵入岩 SHRIMP 锆石 U - Pb 年龄及其深部动力学背景[J]. 中国科学 D 辑: 地球科学, 2008, 38(5): 630 - 645.
Wu G G, Zhang D, Di Y J, et al. The SHRIMP zircon U - Pb ages and deep - seated tectonic background of intrusive rocks in the Tongling mining district[J]. Science China (Earth Sciences), 2008, 38(5): 630 - 645.
- [7] 杨鑫朋, 刘蓓蓓, 程洲, 等. 皖浙赣相邻区构造活动 ESR 测年、Ar - Ar 测年及其构造年代学意义[J]. 中国地质调查, 2022, 9(6): 23 - 32.
Yang X P, Liu B B, Cheng Z, et al. ESR dating, Ar - Ar dating and its tectonic implications of tectonic activity in adjacent area of Anhui - Zhejiang - Jiangxi[J]. Geological Survey of China, 2022, 9(6): 23 - 32.
- [8] Yan J, Liu J M, Li Q Z, et al. In situ zircon Hf - O isotopic analyses of late Mesozoic magmatic rocks in the Lower Yangtze River Belt, central eastern China: Implications for petrogenesis and geodynamic evolution[J]. Lithos, 2015, 227: 57 - 76.
- [9] 常印佛, 刘湘培, 吴言昌. 长江中下游铜铁成矿带[M]. 北京: 地质出版社, 1991: 71 - 76.
Chang Y F, Liu X P, Wu Y C. The Copper - Iron mineralization Belt in the Middle - Lower Reaches of the Yangtze River[M]. Beijing: Geological Publishing House, 1991: 71 - 76.
- [10] 闫峻, 后田结, 王爱国, 等. 皖南中生代早期成矿和晚期非成矿花岗岩成因对比[J]. 中国科学: 地球科学, 2017, 47(11): 1269 - 1291.
Yan J, Hou T J, Wang A G, et al. Petrogenetic contrastive studies on the Mesozoic early stage ore - bearing and late stage ore - barren granites from the southern Anhui Province[J]. Science China Earth Sciences, 2017, 60(11): 1920 - 1941.
- [11] 聂张星, 石磊, 古黄玲, 等. 江南过渡带东至查册桥金矿床 $^{40}\text{Ar} - ^{39}\text{Ar}$ 年代学及成矿条件研究[J]. 大地构造与成矿学, 2017, 41(3): 502 - 515.
Nie Z X, Shi L, Gu H L, et al. $^{40}\text{Ar} - ^{39}\text{Ar}$ geochronology and its geological significance of Zhaceqiao gold deposit in Dongzhi, Jiangnan transition zone[J]. Geotectonica et Metallogenia, 2017, 41(3): 502 - 515.
- [12] 闫峻, 刘海泉, 宋传中, 等. 长江中下游繁昌 - 宁芜火山盆地火山岩锆石 U - Pb 年代学及其地质意义[J]. 科学通报, 2009, 54(12): 1716 - 1724.
Yan J, Liu H Q, Song C Z, et al. Zircon U - Pb geochronology of the volcanic rocks from Fanchang - Ningwu volcanic basins in the Lower Yangtze region and its geological implications[J]. Chinese Science Bulletin, 2009, 54(16): 2895 - 2904.
- [13] 闫峻. 长江中下游 - 大别造山带中生代火山岩特征及成因[J]. 华东地质, 2022, 43(4): 375 - 390.
Yan J. Characteristics and petrogenesis of the Mesozoic volcanic rocks from the Middle - Lower Yangtze River Belt and the Dabie Orogen[J]. East China Geology, 2022, 43(4): 375 - 390.
- [14] Chen L, Zhao Z F, Zheng Y F. Origin of andesitic rocks: Geochemical constraints from Mesozoic volcanics in the Luzong basin, South China[J]. Lithos, 2014, 190 - 191: 220 - 239.
- [15] Chen L, Zheng Y F, Zhao Z F. Geochemical constraints on the origin of Late Mesozoic andesites from the Ningwu basin in the Middle - Lower Yangtze Valley, South China[J]. Lithos, 2016, 254 - 255: 94 - 117.
- [16] 薛怀民. 长江中下游火山岩带东南缘溧阳盆地火山作用的年代学、地球化学及岩浆成因探讨[J]. 地球化学, 2016, 45(3): 213 - 234.
Xue H M. Geochronology, geochemistry and petrogenesis of volcanism in the Liyang volcanic basin on the southeastern margin of the Middle - Lower Yangtze region[J]. Geochimica, 2016, 45(3): 213 - 234.
- [17] 王存智, 黄志忠, 赵希林, 等. 长江中下游宣城水东地区早白垩世酸性火山岩年代学、地球化学及岩石成因[J]. 岩石矿物学杂志, 2018, 37(5): 697 - 715.
Wang C Z, Huang Z Z, Zhao X L, et al. Geochronology, geochemistry and petrogenesis of Early Cretaceous acid volcanic rocks in Shuidong area, Xuancheng City, in the middle - lower reaches of the Yangtze River[J]. Acta Petrologica et Mineralogica, 2018, 37(5): 697 - 715.
- [18] 周涛发, 范裕, 袁峰. 长江中下游成矿带成岩成矿作用研究进展[J]. 岩石学报, 2008, 24(8): 1665 - 1678.
Zhou T F, Fan Y, Yuan F. Advances on petrogenesis and metallogeny study of the mineralization belt of the Middle and Lower Reaches of the Yangtze River area[J]. Acta Petrologica Sinica, 2008, 24(8): 1665 - 1678.
- [19] Song G X, Qin K Z, Li G M, et al. Mesozoic magmatism and metallogeny in the Chizhou area, Middle - Lower Yangtze Valley, SE China: Constrained by petrochemistry, geochemistry and geochro-

- nology[J]. *Journal of Asian Earth Sciences*, 2014, 91: 137 – 153.
- [20] Liu Y S, Hu Z C, Gao S, et al. In situ analysis of major and trace elements of anhydrous minerals by LA – ICP – MS without applying an internal standard [J]. *Chemical Geology*, 2008, 257 (1 – 2): 34 – 43.
- [21] Liu Y S, Gao S, Hu Z C, et al. Continental and oceanic crust recycling – induced melt – peridotite interactions in the Trans – North China Orogen: U – Pb dating, Hf isotopes and trace elements in zircons from mantle xenoliths [J]. *Journal of Petrology*, 2010, 51 (1/2): 537 – 571.
- [22] Ludwig K R. *Isoplot/EX Version 2.49: A Geochronological Toolkit for Microsoft Excel* [M]. Berkeley: Berkeley Geochronology Center Special Publication, 2003, 1a: 1 – 56.
- [23] Scherer E, Munker C, Mezger K. Calibration of the lutetium – hafnium clock [J]. *Science*, 2001, 293 (5530): 683 – 687.
- [24] Blichert – Toft J, Albarède F. The Lu – Hf isotope geochemistry of chondrites and the evolution of the mantle – crust system [J]. *Earth and Planetary Science Letters*, 1997, 148 (1 – 2): 243 – 258.
- [25] Vervoort J D, Blichert – Toft J. Evolution of the depleted mantle: Hf isotope evidence from juvenile rocks through time [J]. *Geochimica et Cosmochimica Acta*, 1999, 63 (3 – 4): 533 – 556.
- [26] Griffin W L, Wang X, Jackson S E, et al. Zircon chemistry and magma mixing, SE China: In – situ analysis of Hf isotopes, Tonglu and Pingtan igneous complexes [J]. *Lithos*, 2002, 61 (3 – 4): 237 – 269.
- [27] 毛景文, 谢桂青, 李晓峰, 等. 大陆动力学演化与成矿研究: 历史与现状——兼论华南地区在地质历史演化期间大陆增生与成矿作用 [J]. *矿床地质*, 2005, 24 (3): 193 – 205.
- Mao J W, Xie G Q, Li X F, et al. Geodynamic process and metallogeny: History and present research trend, with a special discussion on continental accretion and related metallogeny throughout geological history in South China [J]. *Mineral Deposits*, 2005, 24 (3): 193 – 205.
- [28] Wang Q, Wyman D A, Xu J F, et al. Early Cretaceous adakitic granites in the Northern Dabie Complex, central China: Implications for partial melting and delamination of thickened lower crust [J]. *Geochimica Et Cosmochimica Acta*, 2007, 71 (10): 2609 – 2636.
- [29] Liu S A, Li S G, He Y S, et al. Geochemical contrasts between early Cretaceous ore – bearing and ore – barren high – Mg adakites in central – eastern China: Implications for petrogenesis and Cu – Au mineralization [J]. *Geochimica Et Cosmochimica Acta*, 2010, 74 (24): 7160 – 7178.
- [30] Mao J W, Xie G Q, Duan C, et al. A tectono – genetic model for porphyry – skarn – stratabound Cu – Au – Mo – Fe and magnetite – apatite deposits along the Middle – Lower Yangtze River Valley, Eastern China [J]. *Ore Geology Reviews*, 2011, 43 (1): 294 – 314.
- [31] Xie J C, Yang X Y, Sun W D, et al. Early Cretaceous dioritic rocks in the Tongling region, eastern China: Implications for the tectonic settings [J]. *Lithos*, 2012, 150: 49 – 61.
- [32] Li X H, Li Z X, Li W X, et al. Revisiting the “C – type adakites” of the Lower Yangtze River Belt, central eastern China: In – situ zircon Hf – O isotope and geochemical constraints [J]. *Chemical Geology*, 2013, 345: 1 – 15.
- [33] 吴才来, 郭祥焱, 王次松, 等. 铜陵地区高钾钙碱性系列侵入岩锆石 U – Pb 年代学及其地质意义 [J]. *地球化学*, 2013, 42 (1): 11 – 28.
- Wu C L, Guo X Y, Wang C S, et al. Zircon U – Pb dating of high – K calc – alkaline intrusive rocks from Tongling: Implications for the tectonic setting [J]. *Geochimica*, 2013, 42 (1): 11 – 28.
- [34] Wang S W, Zhou T F, Yuan F, et al. Geological and geochemical studies of the Shuijadian porphyry Cu deposit, Anhui Province, Eastern China: Implications for ore genesis [J]. *Journal of Asian Earth Sciences*, 2015, 103: 252 – 275.
- [35] 袁峰, 周涛发, 范裕, 等. 安徽繁昌盆地中生代火山岩锆石 LA – ICP MS U – Pb 年龄及其意义 [J]. *岩石学报*, 2010, 26 (9): 2805 – 2817.
- Yuan F, Zhou T F, Fan Y, et al. LA – ICPMS U – Pb ages of zircons from Mesozoic volcanic rocks and their significance in Fanchang basin, Anhui Province, China [J]. *Acta Petrologica Sinica*, 2010, 26 (9): 2805 – 2817.
- [36] 杜玉雕, 魏国辉. 安徽庐枞盆地枞阳地区玄武质火山岩地球化学特征及其地质意义 [J]. *华东地质*, 2019, 40 (3): 188 – 198.
- Du Y D, Wei G H. Geochemical characteristics and geological significance of the basaltic volcanic rocks in the Zongyang area of Luzong Basin, Anhui Province [J]. *East China Geology*, 2019, 40 (3): 188 – 198.
- [37] Wu F Y, Ji W Q, Sun D H, et al. Zircon U – Pb geochronology and Hf isotopic compositions of the Mesozoic granites in southern Anhui Province, China [J]. *Lithos*, 2012, 150: 6 – 25.
- [38] 王小龙, 曾键年, 马昌前, 等. 宁镇地区燕山期侵入岩锆石 U – Pb 定年: 长江中下游新一期成岩成矿作用的年代学证据 [J]. *地学前缘*, 2014, 21 (6): 289 – 301.
- Wang X L, Zeng J N, Ma C Q, et al. Zircon U – Pb dating of Yan-shanian intrusive rocks in Ningzhen District, Jiangsu: The chronology evidence for a new stage of petrogenesis and metallogeny in the Middle and Lower Reaches of Yangtze River [J]. *Earth Science Frontiers*, 2014, 21 (6): 289 – 301.
- [39] Wang Q, Wyman D A, Xu J F, et al. Petrogenesis of Cretaceous adakitic and shoshonitic igneous rocks in the Luzong area, Anhui Province (eastern China): Implications for geodynamics and Cu – Au mineralization [J]. *Lithos*, 2006, 89 (344): 424 – 446.
- [40] Zhang S B, Zheng Y F, Wu Y B, et al. Zircon isotope evidence for ≥ 3.5 Ga continental crust in the Yangtze craton of China [J]. *Precambrian Research*, 2006, 146 (1/2): 16 – 34.
- [41] Zhang S B, Zheng Y F. Formation and evolution of Precambrian continental lithosphere in South China [J]. *Gondwana Research*, 2013, 23 (4): 1241 – 1260.
- [42] 邢凤鸣, 徐祥, 李志昌. 长江中下游早元古代基底的存在及意义 [J]. *科学通报*, 1993, 38 (20): 1883 – 1886.

- [43] Grimmer J C, Ratschbacher L, McWilliams M, et al. When did the ultrahigh - pressure rocks reach the surface? A $^{207}\text{Pb}/^{206}\text{Pb}$ zircon, $^{40}\text{Ar}/^{39}\text{Ar}$ white mica, Si - in - white mica, single - grain provenance study of Dabie Shan synorogenic foreland sediments [J]. *Chemical Geology*, 2003, 197(1/2/3/4): 87 - 110.
- [44] Guo J L, Gao S, Wu Y B, et al. 3.45 Ga granitic gneisses from the Yangtze Craton, South China: Implications for Early Archean crustal growth [J]. *Precambrian Research*, 2014, 242: 82 - 95.
- [45] Zhang S B, He Q, Zheng Y F. Geochronological and geochemical evidence for the nature of the Dongling Complex in South China [J]. *Precambrian Research*, 2015, 256: 17 - 30.
- [46] Wang X L, Zhou J C, Wan Y S, et al. Magmatic evolution and crustal recycling for Neoproterozoic strongly peraluminous granitoids from southern China: Hf and O isotopes in zircon [J]. *Earth and Planetary Science Letters*, 2013, 366: 71 - 82.
- [47] 李武显, 周新民, 李献华, 等. 庐山“星子变质核杂岩”中伟晶岩锆石 U - Pb 年龄及其地质意义 [J]. *地球科学*, 2001, 26(5): 491 - 495.
Li W X, Zhou X M, Li X H, et al. Zircon U - Pb dating of pegmatite from Xingzi metamorphic core complex of Lushan mountain and its geological implication [J]. *Earth Science*, 2001, 26(5): 491 - 495.
- [48] 朱清波, 杨坤光, 王艳. 庐山变质核杂岩伸展拆离和岩浆作用的年代学约束 [J]. *大地构造与成矿*, 2010, 34(3): 391 - 401.
Zhu Q B, Yang K G, Wang Y. Extensional detachment and magmatism of the Lushan metamorphic core complex: Constraints from $^{40}\text{Ar}/^{39}\text{Ar}$ and U - Pb geochronology [J]. *Geotectonica et Metallogenia*, 2010, 34(3): 391 - 401.
- [49] 关俊朋, 何斌, 李德威. 庐山地区星子群碎屑锆石 SIMS U - Pb 年龄及其地质意义 [J]. *大地构造与成矿*, 2010, 34(3): 402 - 407.
Guan J P, He B, Li D W. SIMS U - Pb dating of the detrital zircons from the Xingzi Group in Lushan area and its geological significance [J]. *Geotectonica et Metallogenia*, 2010, 34(3): 402 - 407.
- [50] 尹国胜, 谢国刚. 江西庐山地区伸展构造与星子变质核杂岩 [J]. *中国区域地质*, 1996(1): 17 - 26.
Yin G S, Xie G G. Extensional structure and the Xingzi metamorphic core complex in the Lushan area, Jiangxi [J]. *Regional Geology of China*, 1996(1): 17 - 26.

The constraints of captured zircon ages from Mesozoic diorite porphyrite vein in Guichi area of Anhui Province on the basement nature of Jiangnan transitional zone

WANG Cunzhi, ZHANG Xiang, HUANG Zhizhong, SONG Shiming, JU Dongmei, CHU Pingli
(Nanjing Center, China Geological Survey, Jiangsu Nanjing 210016, China)

Abstract: Jiangnan transitional zone is located in the northern margin of Jiangnan Orogenic belt of the lower Yangtze area. In order to investigate the basal nature of Jiangnan transitional zone, the authors conducted U - Pb chronology and Hf isotope analysis on captured zircons developed in the Mesozoic diorite porphyrite vein of Huazhili village in Guizhi area. The results show that these zircons have a relatively scattered age distribution, and the age - weighted average of the five primary zircons is (147.7 ± 2.2) Ma, indicating the age of the vein formation. Except for the oldest one with the age of (3263 ± 44) Ma, the captured zircon ages are mainly distributed in 850 ~ 712 Ma, 1346 ~ 1139 Ma, 2283 ~ 1828 Ma and 2944 ~ 2302 Ma, which are consistent with the distribution ages of detrital zircons in Dongling Group of middle and lower reaches of Changjiang River. The zircon Hf isotopic compositions are similar to those in Dongling Group and Kongling Group rocks, which are different from the basement rocks of Jiangnan orogenic belt, indicating the existence of “Jiangbei” basement in this area. At the same time, Changzhou - Chongyang Fault cannot be used as the boundary between “Jiangbei” and “Jiangnan” basement in Lower Yangtze area, and it is predicted that the boundary is located in Jiangnan Fault, which is more to the south. This new understanding helps us to deepen our understanding of the tectonic pattern of Lower Yangtze area.

Keywords: Jiangnan transitional zone; basement nature; diorite porphyrite vein; zircon U - Pb chronology; Hf isotope